

Compressed Sensing for brain MRIs

¹Xiaowei Tong, ¹Jie Han

(¹School of Information Technology, Suzhou University, Suzhou, 215000, China)

Email: jiehan.suda@gmail.com

Abstract: Compressed sensing and magnetic resonance imaging are hot topics in the field of signal processing. In this study we introduced in Lustig's variable density sampling method, integrated it to compressed sensing, and applied it to brain MRI acquisition. The realistic experiment shows the variable density sampling recovery better than traditional random sampling method on a 256x256 brain magnetic resonance image at acceleration factor as 3.

Keyword: Compressed Sensing; brain MRIs; Variable Density Sampling; Random Sampling

1 Introduction

MRI is a medical imaging technique used in radiology to visualize detailed internal structures [1]. It makes use of the property of nuclear magnetic resonance (NMR) to image nuclei of atoms inside the body. It provides good contrast between the different soft tissues of the body, which makes it especially useful in imaging the brain, muscles, the heart, and cancers compared with other medical imaging techniques such as CT or X-rays. Unlike CT scans or X-rays, MRI uses no ionizing radiation. Compressed sensing (CS) is a technique for acquiring and reconstructing a signal utilizing the prior knowledge that it is sparse or compressible. The field has existed for at least four decades, but recently the field has exploded [2]. A precursor to compressed sensing was first used in the 1970s, when seismologists constructed images of reflective layers within the earth based on data that did not seem to satisfy the Nyquist–Shannon criterion [3]. The ideas behind compressive sensing came together in or about 2004 when David Donoho discovered important results on the minimum number of data needed to reconstruct an image even though the number data would be deemed insufficient by the Nyquist–Shannon criterion [4].

There is a tendency for scholars to apply CS in the field of MRI to accelerate the scan. Zhang et al. [5] proposed a novel two-level iterative reconstruction method for compressed sensing magnetic resonance imaging. For the model of this method, they incorporated the phase correction matrix and region of support (ROS) to guarantee more accurate reconstruction. For the algorithm of the method, they proposed an iterative strategy to reduce memory and computation time, and a two-level strategy to take into account both low and high frequency k -space data separately. Their simulation results on normal brain image and angiogram of cerebral demonstrated that the median square error of this proposed method was much less than the traditional method. The error reduction ratios are 11.94% for brain image and 4.53% for angiogram of cerebral, respectively.

Paulsen et al. [6] proposed that NMR can probe the microstructures of anisotropic materials such as liquid crystals, stretched polymers and biological tissues through measurement of the diffusion propagator, where internal structures are indicated by restricted diffusion. Multi-dimensional measurements can probe the microscopic anisotropy, but full sampling can then quickly become prohibitively time consuming. However, for incompletely sampled data, compressed sensing is an effective reconstruction technique to enable accelerated acquisition. They demonstrate that with a compressed sensing scheme, one can greatly reduce the sampling and the experimental time with minimal effect on the reconstruction of the diffusion propagator with an example of anisotropic diffusion. They compare full sampling down to 64x subsampling for the 2D propagator measurement and reduce the acquisition time for the 3D experiment by a factor of 32 from approximately 80 days to approximately 2.5 days.

Langlet et al. [7] addressed three-dimensional tomographic reconstruction of rotational angiography acquisitions. In clinical routine, angular subsampling commonly occurs, due to the technical limitations of C-arm systems or possible improper injection. Standard methods such as filtered back-projection yield a reconstruction that is deteriorated by sampling artifacts, which potentially hampers medical interpretation. Recent developments of compressed sensing have demonstrated that it is possible to significantly improve reconstruction of sub-sampled datasets by generating sparse approximations through ℓ_1 -penalized minimization. Based on these results, they present an extension of the iterative filtered back-projection that includes a sparsity constraint called soft background subtraction. Their approach was shown to provide sampling artifact reduction when reconstructing sparse objects, and more interestingly, when reconstructing sparse objects over a non-sparse background. The relevance of their approach was evaluated in cone-beam geometry on real clinical data.

Seeger et al. [8] phased the optimization of k -space sampling for nonlinear sparse MRI reconstruction as a Bayesian experimental design problem. Bayesian inference is approximated by a novel relaxation to standard signal

processing primitives, resulting in an efficient optimization algorithm for Cartesian and spiral trajectories. On clinical resolution brain image data from a Siemens 3T scanner, automatically optimized trajectories lead to significantly improved images, compared to standard low-pass, equispaced, or variable density randomized designs. Finally they gave the insights into the nonlinear design optimization problem for MRI.

Doneva et al. [9] found that multi echo chemical shift-based water-fat separation methods allow for uniform fat suppression in the presence of main field inhomogeneities. However, these methods require additional scan time for chemical shift encoding. Their work presented a method for water-fat separation from undersampled data (CS-WF), which combined compressed sensing and chemical shift-based water-fat separation. Undersampling was applied in the k -space and in the chemical shift encoding dimension to reduce the total scanning time. Their method can reconstruct high quality water and fat images in 2D and 3D applications from undersampled data. As an extension, multi-peak fat spectral models were incorporated into the CS-WF reconstruction to improve the water-fat separation quality. In 3D MRI, reduction factors of above three can be achieved, thus fully compensating the additional time needed in three-echo water-fat imaging. Their method was demonstrated on knee and abdominal in vivo data.

Jung et al. [10] proposed a compressed sensing dynamic MR technique called k - t FOCUSS (k - t FOCal Underdetermined System Solver). It outperformed the conventional k - t BLAST/SENSE (Broad-use Linear Acquisition Speed-up Technique/SENSitivity Encoding) technique by exploiting the sparsity of x - f signals. They applied this idea to radial trajectories for high-resolution cardiac cine imaging. Radial trajectories are more suitable for high-resolution dynamic MRI than Cartesian trajectories since there is smaller tradeoff between spatial resolution and number of views if streaking artifacts due to limited views can be resolved. As shown for Cartesian trajectories, k - t FOCUSS algorithm efficiently removes artifacts while preserving high temporal resolution. Their k - t FOCUSS algorithm applied to radial trajectories is expected to enhance dynamic MRI quality. Rather than using an explicit gridding method, which transforms radial k -space sampling data to Cartesian grid prior to applying k - t FOCUSS algorithms, they used implicit gridding during FOCUSS iterations to prevent k -space sampling errors from being propagated. In addition, motion estimation and motion compensation after the first FOCUSS iteration were used to further sparsify the residual image. By applying an additional k - t FOCUSS step to the residual image, improved resolution was achieved. Their in vivo experimental results showed that their method can provide high spatiotemporal resolution even from a very limited radial data set.

Ajraoui et al. [11] applied compressed sensing techniques to the acquisition and reconstruction of hyperpolarized ^3He lung MR images was investigated. The sparsity of ^3He lung images in the wavelet domain was investigated through simulations based on fully sampled

Cartesian two-dimensional and three-dimensional ^3He lung ventilation images, and the k -spaces of 2D and 3D images were undersampled randomly and reconstructed by minimizing the L1 norm. Their simulation results showed that temporal resolution can be readily improved by a factor of 2 for two-dimensional and 4 to 5 for three-dimensional ventilation imaging with ^3He with the levels of signal to noise ratio (SNR) (approximately 19) typically obtained. The feasibility of producing accurate functional apparent diffusion coefficient (ADC) maps from undersampled data acquired with fewer radiofrequency pulses was also demonstrated, with the preservation of quantitative information (mean ADC(cs) approximately mean ADC(full) approximately 0.16 cm² sec⁻¹). Prospective acquisition of 2-fold undersampled two-dimensional ^3He images with a compressed sensing k -space pattern was then demonstrated in a healthy volunteer, and the results were compared to the equivalent fully sampled images (SNR(cs) = 34, SNR(full) = 19).

In Hong et al.'s work [12], they found that compressed sensing MRI (CS-MRI) aims to significantly reduce the measurements required for image reconstruction in order to accelerate the overall imaging speed. The sparsity of the MR images in transformation bases is one of the fundamental criteria for CS-MRI performance. Sparser representations can require fewer samples necessary for a successful reconstruction or achieve better reconstruction quality with a given number of samples. Generally, there are two kinds of sparsifying transforms: predefined transforms and data-adaptive transforms. The predefined transforms, such as the discrete cosine transform, discrete wavelet transform and identity transform have usually been used to provide sufficiently sparse representations for limited types of MR images, in view of their isolation to the object images. They presented the singular value decomposition (SVD) as the data-adaptive sparsity basis, which can sparsify a broader range of MR images and perform effective image reconstruction. The performance of their method was evaluated for MR images with varying content (for example, brain images, angiograms, etc), in terms of image quality, reconstruction time, sparsity and data fidelity. Comparison with other commonly used sparsifying transforms showed that their proposed method can significantly accelerate the reconstruction process and still achieve better image quality, providing a simple and effective alternative solution in the CS-MRI framework.

In this paper, we introduced the Variance Density Sampling (VDS) technique to accelerate the CS recovery. Compared to Random Sampling (RS) technique, the VDS is more robust and faster. The structure of this paper is designed as follows. Next section 2 introduces the basic of MRI & CS. Section 3 introduced in the variable density sampling. Section 4 is the experiments, demonstrating the superiority of VDS to RS, and section 5 concludes the paper.

2 Method

2.1 NMR

Nuclear magnetic resonance (NMR) is a physical phenomenon in which magnetic nuclei in a magnetic field absorb and re-emit electromagnetic radiation. This energy is at a specific resonance frequency which depends on the strength of the magnetic field and the magnetic properties of the isotope of the atoms [13-15]. NMR allows the observation of specific quantum mechanical magnetic properties of the atomic nucleus. Many scientific techniques exploit NMR phenomena to study molecular physics, crystals, and non-crystalline materials through NMR spectroscopy. NMR is also routinely used in advanced medical imaging techniques, especially in magnetic resonance imaging (MRI).

All isotopes containing an odd number of protons and of neutrons have an intrinsic magnetic moment and angular momentum, viz., a nonzero spin, while all nuclides with even numbers of both have a total spin of zero. The most commonly studied nuclei are ^1H and ^{13}C , although nuclei from isotopes of many other elements have been studied by high-field NMR spectroscopy as well. The key feature of NMR is that the resonance frequency of a particular substance is directly proportional to the strength of the applied magnetic field. This feature exploits in imaging techniques; if a sample is placed in a non-uniform magnetic field then the resonance frequencies of the sample's nuclei depend on where in the field they are located. The resolution of the imaging technique depends on the magnitude of magnetic field gradient, so many efforts are made to develop increased field strength, often using superconductors. The effectiveness of NMR can also be improved using hyper-polarization, and using 2D, 3D and higher-dimensional multi-frequency techniques [16-18].

2.2 MRI

MRI is a medical imaging technique used in radiology to visualize detailed internal structures. It makes use of the property of NMR to image nuclei of atoms inside the body. an imaging technique that produces high quality images of the anatomical structures of the human body [19-22]. The diagnostic values of MRI are greatly magnified by the automated and accurate classification of the MR images [23-24]. In this paper, our research focuses on developing an automatic method that can distinguish the normal and abnormal MRI brain image. It provides good contrast between the different soft tissues of the body, which makes it especially useful in imaging the brain, heart, muscles, and cancers compared with other medical imaging techniques such as CT or X-rays. Unlike CT scans or traditional X-rays, MRI does not use ionizing radiation. Fig. 1 gives an illustration of an MRI scanner.

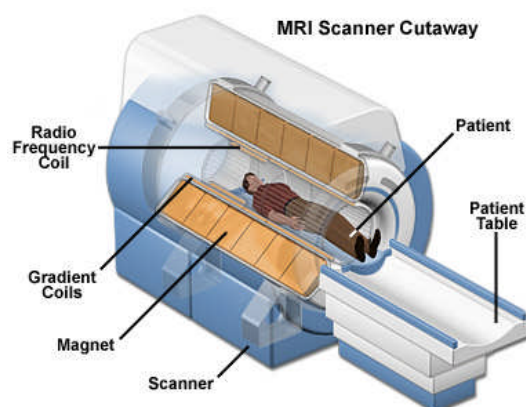


Fig. 1 An MRI Scanner

The body is largely composed of water molecules. Each water molecule has two hydrogen nuclei. When a person is inside the magnetic field, the average magnetic moment of many protons becomes aligned with the direction of the field. A radio frequency transmitter is briefly turned on, producing a varying electromagnetic field. This electromagnetic field has just the right resonance frequency to be absorbed and flip the spin of the protons in the magnetic field. After the electromagnetic field is turned off, the spins of the protons return to thermodynamic equilibrium and the bulk magnetization becomes re-aligned with the static magnetic field. During this relaxation, a radio frequency signal is generated, which can be measured with receive coils [25-26].

Protons in different tissues return to their equilibrium state at different relaxation rates. By changing the settings on the scanner, this effect is used to create contrast between different areas of body tissue. Contrast agents may be injected to enhance the appearance of blood vessels, tumors or inflammation. They may also be directly injected into a joint in the case of arthrograms, MRI images of joints. Nonetheless the strong magnetic fields and radio pulses can affect metal implants, including cochlear implants and cardiac pacemakers.

2.3 Compressed Sensing

CS is a technique for finding sparse solutions to underdetermined linear systems, which has more unknowns than equations and generally has an infinite number of solutions. However, if there is a unique sparse solution to the underdetermined system, then the CS allows the recovery of that solution. Not all underdetermined systems of linear equations have a sparse solution. CS takes advantage of the redundancy in many of interesting signals. In particular, many signals are sparse, i.e., they contain many coefficients close to or equal to zero, when represented in some domain [27-29].

In electrical engineering, particularly in signal processing, CS is the process of acquiring and reconstructing a signal that is supposed to be sparse or compressible. The CS requires three conditions [30]: 1) The desired images have a sparse representation; 2) The aliasing

artifacts are incoherent; 3) A nonlinear reconstruction [6, 31-32]. The field of CS is related to other topics in signal processing and computational mathematics, such as to underdetermined linear-systems, group testing, heavy hitters, sparse coding, multiplexing, sparse sampling, and finite rate of innovation. Imaging techniques having a strong affinity with compressive sensing include coded aperture and computational photography.

Starting with the single-pixel camera from Rice University, an up-to-date list of the most recent implementations of compressive sensing in hardware at different technology readiness level is available. Some hardware implementation (like the one used in MRI or compressed genotyping) do not require an actual physical change, whereas other hardware require substantial re-engineering to perform this new type of sampling. Similarly, a number of hardware implementations already existed before 2004; however, while they were acquiring signals in a compressed manner, they generally did not use compressive sensing reconstruction techniques to reconstruct the original signal. The results of these reconstructions were suboptimal and have been greatly enhanced thanks to CS.

2.4 MRI-CS

MRI can be regarded as a special case of CS: Traditional MRI samplings are simply individual Fourier coefficients (k -space samples), and MRI images are sparse in transformed domains such as wavelet; aliasing in randomly undersampled MRI are incoherent [28, 33]. Mathematically, the reconstructions of MRI are obtained by solving the following constrained optimization problem [34-36]

$$\begin{aligned} \min \|\Psi x\|_1 \\ \text{s.t. } \|F_u x - y\|_2 < \varepsilon \end{aligned} \quad (1)$$

where x denotes the signal to be estimated, Ψ denotes the sparse transform matrix, F_u denotes the undersampled Fourier transform, y denotes the measured k -space data from the MRI scanner, and ε controls the fidelity. The objective function in formula (1) is the l_1 norm, which is defined as $\|x\|_1 = \sum_i |x_i|$ that promotes the sparsity when minimized [37]. Fig. 2 shows the flowchart of MRI CS [38].

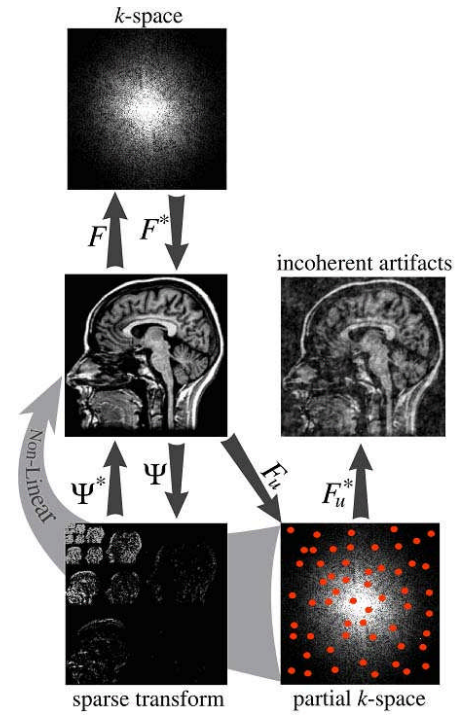


Fig. 2 Flowchart of MRI CS.

2.5 VD Sampling

The incoherence analysis so far assumes the few non-zeros are scattered at random among the entries of the transform domain representation. Representations of natural images exhibit a variety of significant non-random structures. First, most of the energy of images is concentrated close to the k -space origin. Furthermore, using wavelet analysis one can observe that coarse-scale image components tend to be less sparse than fine-scale components [38-39]. Specifically, if k_y and k_x denote the k -space, coefficients in the two phase encoding directions and N and M are the number of phase encoding steps in x and y direction, the PDF was given by

$$PDF = \left(1 - \frac{1}{\sqrt{2NM}} \sqrt{k_x^2 + k_y^2} \right)^p \quad (2)$$

for an appropriately chosen p . The researcher may choose samples randomly with sampling density scaling according to a power of distance from the origin [40-42].

3 Experiments

We compared the introduced VDS-CS method to traditional RS-CS method. The MRI T1 image was acquired by 3T scanner on the brain part of a male patient with 3x acceleration. We chose bior4.4 wavelet, and decompose the image to 4th level. Fig. 3 gives the image, k -space, and wavelet domains.

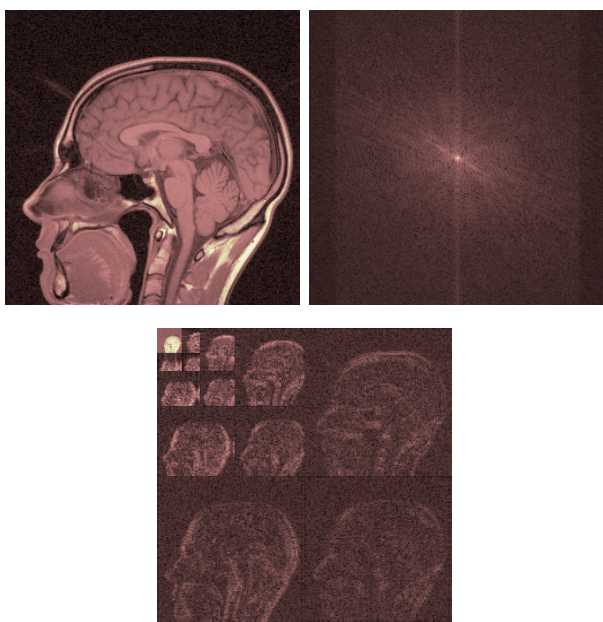


Fig. 3 CS of 256x256 brain T1 image with 4x acceleration: (a) Image domain; (b) K-space domain; (c) Wavelet domain

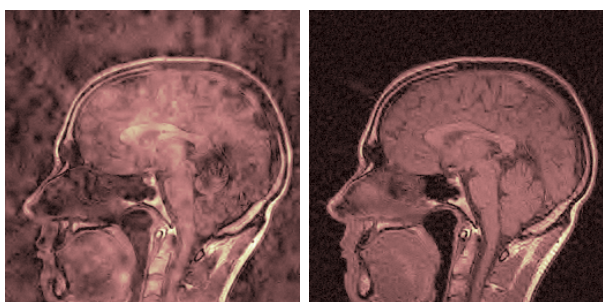


Fig. 4 The recovery Result: (a) Random Sampling; (b) VD Sampling.

Fig. 4 shows the recovery results obtained by RS and VDS. It is clear that VDS-based recovery is better than RS-based recovery. Therefore, we can conclude that the VDS perform better than RS. Fig. 5 gives the convergence curve of the CS algorithm. It shows that the CS got convergence within 50 steps.

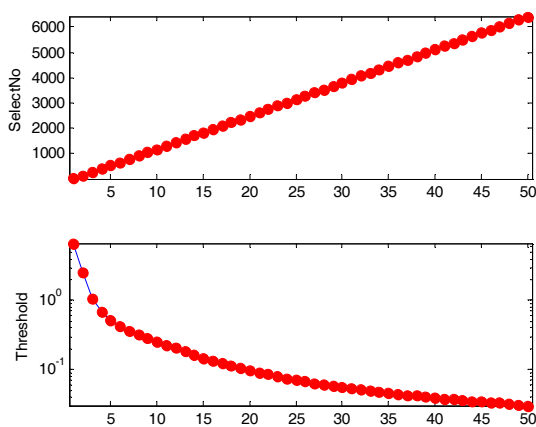


Fig. 5 Convergence of CS

4 Conclusions

In this study, we introduced in and investigated on Lustig's VDS method. The results on a T1 256x256 brain image with acceleration as 3 show that the recovery of VDS is superior to RS, and the convergence of CS is within 50 steps. Next work is to use different image descriptors [43-44] to describe MRI brain images.

References

- [1] Y. Zhang, Z. Dong, L. Wu, S. Wang, A hybrid method for MRI brain image classification, *Expert Systems with Applications*, 38 (2011) 10049-10053.
- [2] C. Nguyen, G.R. Redinbo, Detecting computer-induced errors in remote-sensing JPEG compression algorithms, *IEEE Trans Image Process*, 15 (2006) 1728-1739.
- [3] A. Wagadarikar, R. John, R. Willett, D. Brady, Single disperser design for coded aperture snapshot spectral imaging, *Appl Opt*, 47 (2008) B44-51.
- [4] E.J. Candès, The restricted isometry property and its implications for compressed sensing, *Comptes Rendus Mathématique*, 346 (2008) 589-592.
- [5] Y. Zhang, L. Wu, B. Peterson, z. Dong, A Two-Level Iterative Reconstruction Method for Compressed Sensing MRI, *Journal of Electromagnetic Waves and Applications*, 25 (2011) 1081-1091.
- [6] J.L. Paulsen, H. Cho, G. Cho, Y.Q. Song, Acceleration of multi-dimensional propagator measurements with compressed sensing, *J Magn Reson*, 213 (2011) 166-170.
- [7] H. Langet, C. Riddell, Y. Troussel, A. Tenenhaus, E. Lahalle, G. Fleury, N. Paragios, Compressed sensing based 3D tomographic reconstruction for rotational angiography, *Med Image Comput Comput Assist Interv*, 14 (2011) 97-104.
- [8] M. Seeger, H. Nickisch, R. Pohmann, B. Scholkopf, Optimization of k-space trajectories for compressed sensing by Bayesian experimental design, *Magn Reson Med*, 63 (2010) 116-126.
- [9] M. Doneva, P. Bornert, H. Eggers, A. Mertins, J. Pauly, M. Lustig, Compressed sensing for chemical shift-based water-fat separation, *Magn Reson Med*, 64 (2010) 1749-1759.
- [10] H. Jung, J. Park, J. Yoo, J.C. Ye, Radial k-t FOCUSS for high-resolution cardiac cine MRI, *Magn Reson Med*, 63 (2010) 68-78.
- [11] S. Ajraoui, K.J. Lee, M.H. Deppe, S.R. Parnell, J. Parra-Robles, J.M. Wild, Compressed sensing in hyperpolarized ³He lung MRI, *Magn Reson Med*, 63 (2010) 1059-1069.
- [12] M. Hong, Y. Yu, H. Wang, F. Liu, S. Crozier, Compressed sensing MRI with singular value decomposition-based sparsity basis, *Phys Med Biol*, 56 (2011) 6311-6325.
- [13] Y. Zhang, L. Wu, G. Wei, Color Image Enhancement based on HVS and PCNN, *Science in China E edition: Information Science*, 53 (2010) 1963-1976.
- [14] L. Tasic, R. Rittner, [alpha]-Substituent effects on ¹³C NMR chemical shifts in some aliphatic compounds: Application of principal component analysis (PCA), *Journal of Molecular Structure*, 933 (2009) 15-19.
- [15] I.G. Aursand, U. Erikson, E. Veliyulin, Water properties and salt uptake in Atlantic salmon fillets as affected by ante-mortem stress, rigor mortis, and brine salting: A low-field ¹H NMR and ¹H/²³Na MRI study, *Food Chemistry*, 120 (2010) 482-489.
- [16] H. Metz, K. Mäder, Benchtop-NMR and MRI--A new analytical tool in drug delivery research, *International Journal of Pharmaceutics*, 364 (2008) 170-175.
- [17] Z.I. Cleveland, G.E. Pavlovskaya, K.F. Stupic, J.B. Wooten, J.E. Repine, T. Meersmann, Detection of tobacco smoke deposition by hyperpolarized krypton-83 MRI, *Magnetic Resonance Imaging*, 26 (2008) 270-278.
- [18] Y. Zhang, L. Wu, N. Naggaz, S. Wang, G. Wei, Remote-sensing Image Classification Based on an Improved Probabilistic Neural Network, *Sensors*, 9 (2009) 7516-7539.
- [19] G.A. Wright, Magnetic resonance imaging, *Signal Processing Magazine, IEEE*, 14 (1997) 56-66.
- [20] R.H. Morris, M. Bencsik, N. Nestle, P. Galvosas, D. Fairhurst, A. Vangala, Y. Perrie, G. McHale, Robust spatially resolved pressure

- measurements using MRI with novel buoyant advection-free preparations of stable microbubbles in polysaccharide gels, *Journal of Magnetic Resonance*, 193 (2008) 159-167.
- [21] K. Hynynen, MRI-guided focused ultrasound treatments, *Ultrasonics*, 50 (2010) 221-229.
- [22] S. Bayramoglu, Ö. Kilickesmez, T. Cimilli, A. Kayhan, G. Yirik, F. Islim, S. Alibek, T2-weighted MRI of the Upper Abdomen:: Comparison of Four Fat-Suppressed T2-weighted Sequences Including PROPELLER (BLADE) Technique, *Academic Radiology*, 17 (2010) 368-374.
- [23] Y. Zhang, S. Wang, L. Wu, A Novel Method for Magnetic Resonance Brain Image Classification based on Adaptive Chaotic PSO, *Progress in Electromagnetics Research*, 109 (2010) 325-343.
- [24] F.P. Bymaster, J.S. Katner, D.L. Nelson, S.K. Hemrick-Luecke, P.G. Threlkeld, J.H. Heiligenstein, S.M. Morin, D.R. Gehlert, K.W. Perry, Atomoxetine Increases Extracellular Levels of Norepinephrine and Dopamine in Prefrontal Cortex of Rat: A Potential Mechanism for Efficacy in Attention Deficit/Hyperactivity Disorder, *Neuropsychopharmacology*, 27 (2002) 699-711.
- [25] S.E. Harms, S.S. Harms, Making Quality Technical Decisions: No Free Lunch in MRI, *Seminars in Breast Disease*, 11 (2008) 51-66.
- [26] Y. Zhang, S. Wang, L. Wu, Y. Huo, Artificial Immune System for Protein folding model, *Journal of Convergence Information Technology*, 6 (2011) 55-61.
- [27] G.H. Chen, J. Tang, S. Leng, Prior Image Constrained Compressed Sensing (PICCS), *Proc Soc Photo Opt Instrum Eng*, 6856 (2008) 685618.
- [28] U. Gamper, P. Boesiger, S. Kozerke, Compressed sensing in dynamic MRI, *Magn Reson Med*, 59 (2008) 365-373.
- [29] Y. Zhang, J. Yan, G. Wei, L. Wu, Find multi-objective paths in stochastic networks via chaotic immune PSO, *Expert Systems with Applications*, 37 (2010) 1911-1919.
- [30] D. Needell, J.A. Tropp, CoSaMP: Iterative signal recovery from incomplete and inaccurate samples, *Applied and Computational Harmonic Analysis*, 26 (2009) 301-321.
- [31] M. Aghagolzadeh, K. Oweiss, Compressed and distributed sensing of neuronal activity for real time spike train decoding, *IEEE Trans Neural Syst Rehabil Eng*, 17 (2009) 116-127.
- [32] Y. Zhang, L. Wu, S. Wang, Magnetic Resonance Brain Image Classification by an Improved Artificial Bee Colony Algorithm, *Progress in Electromagnetics Research*, 116 (2011) 65-79.
- [33] M. Aghagolzadeh, M. Shetliffe, K.G. Oweiss, Impact of compressed sensing of motor cortical activity on spike train decoding in Brain Machine Interfaces, *Conf Proc IEEE Eng Med Biol Soc*, 2008 (2008) 5302-5305.
- [34] W.R. Nitz, Fast and ultrafast non-echo-planar MR imaging techniques, *Eur Radiol*, 12 (2002) 2866-2882.
- [35] Y.C. Kim, S.S. Narayanan, K.S. Nayak, Accelerated three-dimensional upper airway MRI using compressed sensing, *Magn Reson Med*, 61 (2009) 1434-1440.
- [36] Y. Zhang, S. Wang, Y. Huo, L. Wu, Feature Extraction of Brain MRI by Stationary Wavelet Transform and its Applications, *Journal of Biological Systems*, 18 (2010) 115-132.
- [37] D. Li, An improved CS applied for MRI, *International Journal of Research and Reviews in Soft and Intelligent Computing*, 1 (2011) 82-84.
- [38] M. Lustig, D. Donoho, J.M. Pauly, Sparse MRI: The application of compressed sensing for rapid MR imaging, *Magn Reson Med*, 58 (2007) 1182-1195.
- [39] S.S. Vasanawala, M.T. Alley, B.A. Hargreaves, R.A. Barth, J.M. Pauly, M. Lustig, Improved Pediatric MR Imaging with Compressed Sensing, *Radiology*, (2010).
- [40] P. Parasoglou, D. Malioutov, A.J. Sederman, J. Rasburn, H. Powell, L.F. Gladden, A. Blake, M.L. Johns, Quantitative single point imaging with compressed sensing, *J Magn Reson*, 201 (2009) 72-80.
- [41] M. Vorechovský, D. Novák, Correlation control in small-sample Monte Carlo type simulations I: A simulated annealing approach, *Probabilistic Engineering Mechanics*, 24 (2009) 452-462.
- [42] F. Knoll, C. Clason, C. Diwoky, R. Stollberger, Adapted random sampling patterns for accelerated MRI, *Magnetic Resonance Materials in Physics, Biology and Medicine*, (2011) 1-8.
- [43] Y. Zhang, L. Wu, A Rotation Invariant Image Descriptor based on Radon Transform, *International Journal of Digital Content Technology and its Applications*, 5 (2011) 209-217.
- [44] Y. Zhang, L. Wu, Rigid Image Registration by PSOSQP Algorithm, *Advances in Digital Multimedia*, 1 (2012) 4-8.